A Method Extending the Boundary Condition for Analyzing Guided Modes of Dielectric Waveguides of Arbitrary Cross-Sectional Shape

NAGAYOSHI MORITA, MEMBER, IEEE

Abstract—**A method based on the extended boundary condition method is presented for analyzing guided modes of dielectric waveguides of arbitrary cross-sectional shape. Numerical integration needed in this method is only over the boundary periphery line of the waveguide. Nevertheless, it is applicable to the waveguides with any refractive index difference between core and cladding ranging from negligibly small to considerably large difference, as well as to certain types of waveguide with inhomogeneous core. Approximate formulas for the case of weakly guiding are also derivable from the general basic set of equations presented. Numerical examples are given to verify the usefulness and accuracy of this method.**

I. Introduction

WITH THE increasing importance of the role of the open waveguide as the optical to millimeter-wave or microwave guiding structure, a variety of dielectric waveguides with circular and noncircular cross-sectional shapes have appeared and been proposed. In order to investigate the propagation characteristics of guided modes of those waveguides, various types of analysis method have been proposed and used. Typical methods of these are point-matching [1]–[4], mode-matching [5], the method using telegraphist's equations [7], [8], and others [9], as applicable to the homogeneous-core guides, and the method of moments [10], variational method [11]–[13], and finite-element method [14], as applicable also to the inhomogeneous-core guides. (The analyses peculiar to the radially inhomogeneous optical fiber are excluded here.)

All these methods, however, seem to have one or some of drawbacks, such as: 1) inadequate in accuracy, particularly, near cutoff; 2) only usable for some particular cross-sectional shape; 3) only effective to the case of small refractive index difference between core and cladding; 4) require numerical integrations over a cross section; 5) need to take a number of unknowns over a cross-sectional area, etc.

This paper presents a quite general and efficient method based on the extended boundary condition method [15], [16]. This method does not only surmount the aforementioned drawbacks but also has the additional advantage such that the fields in the exterior homogeneous region need not be used (at least directly) and pertinent approximations with very high accuracy can be derived according to the usable conditions.

In order to demonstrate the usefulness and accuracy of the present method, the inhomogeneous circular waveguide, the step-index circular waveguide, and the rectangular waveguide are treated with some typical numerical examples for them.

Manuscript received May 27, 1981; revised August 12, 1981.

The author is with the Department of Communication Engineering, Osaka University, Suita-shi, Osaka 565, Japan.

II. General Equations

Consider the modes propagating in the z-direction with the propagation constant β. All electromagnetic fields of modes are supposed to have the common factor $\exp(j\omega t - j\beta z)$ which is eliminated throughout the paper.

Since the problem of guided modes of a dielectric waveguide has the analogical property with the problem of scattering of the obliquely incident wave by the same dielectric cylinder as the waveguide, we could start from the integral representation of field provided for such scattering problems. Thus, by replacing $\cos\varphi$ with $-\beta/k$ in the first equation of [17, eq. (27)] and using (3) of the same reference, we obtain the following electric field expression in the exterior region:

$$\boldsymbol{E}_e = -\frac{\partial W}{2\pi}\int_C \Big[k(\boldsymbol{i}_{n'}\times\boldsymbol{H}) + j\frac{1}{W}(\boldsymbol{i}_{n'}\times\boldsymbol{E})\times(\nabla'_t + j\beta\boldsymbol{i}_z) + \frac{1}{k}\{(\boldsymbol{i}_{n'}\times\boldsymbol{H})\cdot(\nabla'_t + j\beta\boldsymbol{i}_z)\}(\nabla'_t + j\beta\boldsymbol{i}_z)\Big]\psi_e\, dv' \tag{1}$$

where

$$\nabla_t = \nabla - \boldsymbol{i}_z\partial/\partial z$$
$$\psi_e = K_0(h_e R)$$
$$h_e = \sqrt{\beta^2 - k^2} \tag{2}$$

and where k is the wavenumber of the exterior region of the waveguide, and R is the distance between the observation point and the integration point projected on a z-constant plane. In the derivation of (1), the relation

$$H_0^{(2)}(-jz) = (j2/\pi)K_0(z) \tag{3}$$

is used. Other notations and definitions are as follows (see Fig. 1): i.e., C denotes the boundary line between interior

0018-9480/82/0100-0006$00.75 ©1982 IEEE

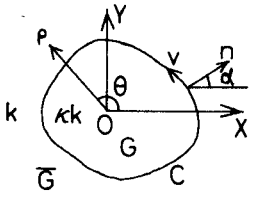

Fig. 1. Cross section of dielectric waveguide and coordinate systems.

(G) and exterior ($\bar{G}$) regions in a cross section; n and v are the coordinates normal to C and along C, respectively, at a point on C; i_a is a unit vector directed along the a-direction, where a stands for some coordinates; α is the angle between i_n and i_x; and W is the wave impedance in region $\bar{G}$. The prime refers to the derivative with respect to the total argument of the indicated function when used on functions, or otherwise refers to the coordinate of the integration point, and the subscript e represents the exterior region.

Using the identity

$$i_x = i_{n'}\cos\alpha' - i_{v'}\sin\alpha' \tag{4}$$

the x-component of (1) becomes

$$E_{ex} = -\frac{jW}{2\pi}\int_c \Big\{ kH_z\sin\alpha' + \beta\cos\alpha'\frac{E_z}{W} - j\sin\alpha'\frac{E_{v'}}{W}\frac{\partial}{\partial n'} - j\cos\alpha'\frac{E_{v'}}{W}\frac{\partial}{\partial v'} - \frac{1}{k}\Big(H_z\frac{\partial}{\partial v'} - j\beta H_{v'}\Big) \cdot\Big(\cos\alpha'\frac{\partial}{\partial n'} - \sin\alpha'\frac{\partial}{\partial v'}\Big)\Big\}\psi_e\, dv'. \tag{5}$$

Note that only tangential components appear in the integrand. Thus, we can replace, using boundary conditions, all fields E_z, H_z, E_v, and H_v by the interior fields E_{iz}, H_{iz}, E_{iv}, and H_{iv}, respectively, where the subscript i represents the interior region. From Maxwell's equations, we get

$$H_{iz} = \frac{j}{kW}\Big(\frac{\partial E_{iv}}{\partial n} - \frac{\partial E_{in}}{\partial v}\Big) \tag{6}$$

$$\frac{\partial H_{iz'}}{\partial v'} + j\beta H_{iv'} = jk\frac{\kappa^2}{W}E_{in'} \tag{7}$$

where κ is the refractive index in G relative to that in $\bar{G}$. Removing magnetic fields from (5) by use of integration by parts, together with (6) and (7), and then removing E_{iz} by use of the equation (see Appendix)

$$j\beta E_{iz} = \frac{2}{\kappa}\Big(\frac{\partial\kappa}{\partial n}E_{in} + \frac{\partial\kappa}{\partial v}E_{iv}\Big) + \frac{\partial E_{in}}{\partial n} + \frac{\partial E_{iv}}{\partial v} \tag{8}$$

(5) reduces to

$$E_{ex} = -\frac{1}{2\pi}\int_c\Big[\frac{\partial E_{ix'}}{\partial n'} - E_{ix'}\frac{\partial}{\partial n'}\Big]\psi_e\, dv' + \frac{1}{2\pi}\int_c\Big[(\kappa^2-1)E_{in'}\Big(\cos\alpha'\frac{\partial}{\partial n'} - \sin\alpha'\frac{\partial}{\partial v'}\Big) - \frac{2}{\kappa}\cos\alpha'\Big(E_{in'}\frac{\partial\kappa}{\partial n'} + E_{iv'}\frac{\partial\kappa}{\partial v'}\Big)\Big]\psi_e\, dv' \tag{9}$$

or

$$E_{ex} = -\frac{1}{2\pi}\int_c\Big[\frac{\partial E_{ix'}}{\partial n'}\psi_e - E_{ix'}\frac{\partial\psi_e}{\partial n'}\Big]dv' + \frac{1}{2\pi}\int_c\Big[(\kappa^2-1)\big(E_{ix'}\cos\alpha' + E_{iy'}\sin\alpha'\big)\frac{\partial\psi_e}{\partial x'} - \frac{2}{\kappa}\cos\alpha'\Big(E_{ix'}\frac{\partial\kappa}{\partial x'} + E_{iy'}\frac{\partial\kappa}{\partial y'}\Big)\psi_e\Big]dv'. \tag{10}$$

Following the similar steps, the expression for E_{ey} reduces to

$$F_{ey} = -\frac{1}{2\pi}\int_c\Big[\frac{\partial E_{iy'}}{\partial n'}\psi_e - E_{iy'}\frac{\partial\psi_e}{\partial n'}\Big]dv' + \frac{1}{2\pi}\int_c\Big[(\kappa^2-1)\big(E_{ix'}\cos\alpha' + E_{iy'}\sin\alpha'\big)\frac{\partial\psi_e}{\partial y'} - \frac{2}{\kappa}\sin\alpha'\Big(E_{ix'}\frac{\partial\kappa}{\partial x'} + E_{iy'}\frac{\partial\kappa}{\partial y'}\Big)\psi_e\Big]dv'. \tag{11}$$

Equations (10) and (11) are the integral expressions of E_{ex} and E_{ey} for the case where the observation point is in the exterior region ($P\in\bar{G}$). On the other hand, if the observation point is placed in the interior region ($P\in G$), both expressions become zero due to the extended boundary condition, which means

$$\text{the right-hand sides of (10) and (11)} = 0, \qquad P\in G. \tag{12}$$

Next, use is made in (12) of the addition theorem of the modified Bessel function

$$\psi_e = \sum_{l=0}^{\infty}\epsilon_l K_l(h_e\rho')I_l(h_e\rho)\cos l(\theta'-\theta), \qquad \rho<\rho' \tag{13}$$

where $\epsilon_l = 2$ unless $l=0$, in which case $\epsilon_l = 1$. Finally, we have the following two basic equations:

$$\int_c\Big\{\Big(\frac{\partial E_{ix'}}{\partial n'} - E_{ix'}\frac{\partial}{\partial n'}\Big) - (\kappa^2-1)\Big(E_{ix'}\cos\alpha' + E_{iy'}\sin\alpha'\Big)\frac{\partial}{\partial x'} + \frac{2}{\kappa}\cos\alpha'\Big(E_{ix'}\frac{\partial\kappa}{\partial x'} + E_{iy'}\frac{\partial x'}{\partial y'}\Big)\Big\} \cdot K_l(h_e\rho')\cos l(\theta'-\theta)\, dv' = 0, \qquad l=0,1,2,\cdots \tag{14}$$

$$\int_c\Big\{\Big(\frac{\partial E_{iy'}}{\partial n'} - E_{iy'}\frac{\partial}{\partial n'}\Big) - (\kappa^2-1)\Big(E_{ix'}\cos\alpha' + E_{iy'}\sin\alpha'\Big)\frac{\partial}{\partial y'} + \frac{2}{\kappa}\sin\alpha'\Big(E_{ix'}\frac{\partial\kappa}{\partial x'} + E_{iy'}\frac{\partial\kappa}{\partial y'}\Big)\Big\} \cdot K_l(h_e\rho')\cos l(\theta'-\theta)\, dv' = 0, \qquad l=0,1,2,\cdots \tag{15}$$

which determine the propagation constants β and the transverse field distributions E_{ix} and E_{iy} of guided modes. All other interior field components can be determined from E_{ix} and E_{iy}, and the electric fields of the exterior region could be obtained from (10) and (11).

Use of the principle of (12) and the identity (13) is the

essential procedure of the extended boundary condition (or null-field, or T-matrix) method [16]. Equations (14) and (15) are not necessarily correct analytically, because of the use of (13); for example, they may not work for a guide with an eccentric cross-sectional shape far different from circle, like strongly concave. However, as long as we treat the "ordinary" dielectric waveguides and we can use the pertinent expressions for E_{lx} and E_{ly}, (14) and (15) could be considered to be the exact equations. Note that (14) and (15) are applicable to the waveguides with the inhomogeneous core region as well as with the arbitrary cross-sectional shape.

III. Inhomogeneous Circular Waveguide

As a first example, let us consider a circular waveguide whose refractive index distribution is given as

$$\kappa^2=\kappa_0^2\{1-h(\rho)\}, \qquad \rho\leqslant a$$
$$=1, \qquad \rho>a. \tag{16}$$

It seems not so easy to get the exact field distributions in the inhomogeneous region $\rho\leqslant a$. Fortunately, however, an approximation is available for the case of weak inhomogeneity; according to this approximation, the electric fields of HE and EH modes in $\rho\leqslant a$ are neatly expressed as [17]–[20]

even HE_{nm}:

$$\boldsymbol{E}_{nm}=A\Omega^{(n-1)}(\rho)\{\boldsymbol{i}_x\cos(n-1)\theta-\boldsymbol{i}_y\sin(n-1)\theta\}$$

odd HE_{nm}:

$$\boldsymbol{E}_{nm}=A\Omega^{(n-1)}(\rho)\{\boldsymbol{i}_x\sin(n-1)\theta+\boldsymbol{i}_y\cos(n-1)\theta\} \tag{17}$$

even EH_{nm}:

$$\boldsymbol{E}_{nm}=A\Omega^{(n+1)}(\rho)\{\boldsymbol{i}_x\cos(n+1)\theta+\boldsymbol{i}_y\sin(n+1)\theta\}$$

odd EH_{nm}:

$$\boldsymbol{E}_{nm}=A\Omega^{(n+1)}(\rho)\{\boldsymbol{i}_x\sin(n+1)\theta-\boldsymbol{i}_y\cos(n+1)\theta\} \tag{18}$$

where the terms even and odd mean the symmetrical property with respect to the x-axis, and $n\geqslant 1$ in general; but the case of $n=0$ is special in that even EH_{0m} tends to TM_{0m} and odd EH_{0m} to TE_{0m}. The integer n used here should not be confused with the coordinate n normal to a point on C. A simple solution of $\Omega^{(n)}(\rho)$ in (17) and (18) will be a solution of the differential equation

$$\left[\frac{d^2}{d\rho^2}+\frac{1}{\rho}\frac{d}{d\rho}+\left\{k^2\kappa_0^2(\chi-h(\rho))-\frac{n^2}{\rho^2}\right\}\right]\Omega^{(n)}(\rho)=0 \tag{19}$$

with

$$\chi=1-\beta^2/k^2\kappa_0^2. \tag{20}$$

A method of solving (19) for general $h(\rho)$ is, for example, described in [19].

The characteristic equations for HE_{nm} and EH_{nm} modes can be derived by substituting electric fields (17) and (18) into (14) or (15). Both even and odd cases result in the same equations except for the case $n=0$, from which case TE and TM modes result

$$HE_{nm}: \left[\frac{\Omega^{(n-1)\prime}(\rho)}{\Omega^{(n-1)}(\rho)}-\frac{\kappa^2+1}{2}h_e\frac{K'_{n-1}(h_e\rho)}{K_{n-1}(h_e\rho)}+\frac{n-1}{2a}(\kappa^2-1)+\frac{1}{\kappa}\frac{d\kappa}{d\rho}\right]_{\rho=a.}=0, \qquad n\geqslant 1 \tag{21}$$

$$EH_{nm}: \left[\frac{\Omega^{(n+1)\prime}(\rho)}{\Omega^{(n+1)}(\rho)}-\frac{\kappa^2+1}{2}h_e\frac{K'_{n+1}(h_e\rho)}{K_{n+1}(h_e\rho)}-\frac{n+1}{2a}(\kappa^2-1)+\frac{1}{\kappa}\frac{d\kappa}{d\rho}\right]_{\rho=a}=0, \qquad n\geqslant 1 \tag{22}$$

$$TE_{0m}: \left[\frac{\Omega^{(1)\prime}(\rho)}{\Omega^{(1)}(\rho)}-h_e\frac{K'_1(h_e\rho)}{K_1(h_e\rho)}\right]_{\rho=a}=0 \tag{23}$$

$$TM_{0m}: \left[\frac{\Omega^{(1)\prime}(\rho)}{\Omega^{(1)}(\rho)}-\kappa^2h_e\frac{K'_1(h_e\rho)}{K_1(h_e\rho)}-\frac{\kappa^2-1}{a}+\frac{2}{\kappa}\frac{\partial\kappa}{\partial\rho}\right]_{\rho=a}=0. \tag{24}$$

These approximate characteristic equations can present solutions with almost the same level of accuracy as of [19], in spite of their far simpler forms. Furthermore, it is quite interesting to notice that the characteristic equations (21)–(24) are just the same equations as those of [21] in which a different approach is employed.

Next, we shall proceed to a simple numerical example. Fig. 2 shows some of the dispersion curves obtained using (21)–(24) for the case of quadratical inhomogeneity given for

$$h(\rho)=d(\rho/a)^2 \tag{25}$$

in which case the solution of (19) can be written as

$$\Omega_\nu^{(n)}(\rho)=\left(\frac{\rho}{s_0}\right)^n\exp\left\{-\frac{1}{2}\left(\frac{\rho}{s_0}\right)^2\right\}L_\nu^{(n)}\left(\frac{\rho^2}{s_0^2}\right) \tag{26}$$

where

$$\nu=-\frac{1}{2}\left\{n+1-\frac{1}{2}s_0^2\left(k^2\kappa_0^2-\beta^2\right)\right\}$$
$$s_0^2=a/\left(k\kappa_0\sqrt{d}\right) \tag{27}$$

and $L_\nu^{(n)}(\cdot)$ is the Laguerre function. One of the abscissas V is the normalized frequency $ka\sqrt{2\kappa_0(\kappa_0-1)}$. Examples for three different values of d are shown in which the case $d=0$ corresponds to a step-index fiber, while the case $d=0.015$ corresponds to a fiber with smaller refractive index in the core region near cladding than that in the

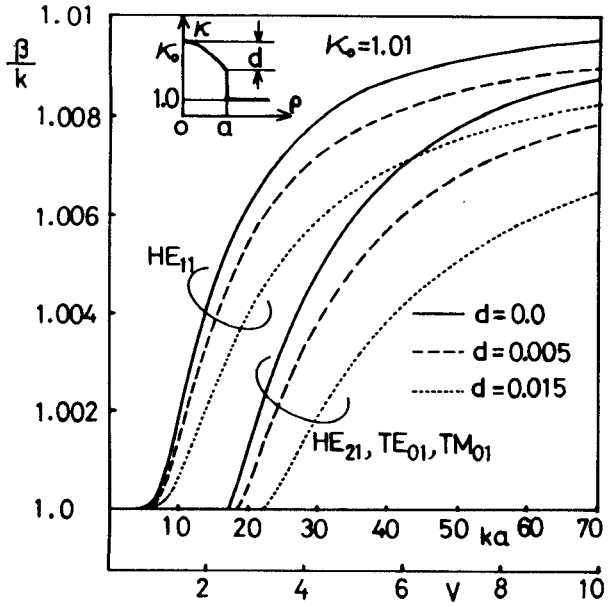

Fig. 2. Dispersion curves of quadratically inhomogeneous circular dielectric waveguide. $\kappa_0 = 1.01$.

cladding. We can notice at a glance the marked effect of d on widening the single-mode frequency region. Differences among HE_{21}, TE_{01}, and TM_{01} modes cannot be discriminated on this graph. It is checked that each curve perfectly agrees with that of the corresponding mode obtained from the characteristic equation of [19].

Although the results of this section may not be necessarily new, the equations given in this section shall be found soon to be connected to and useful for the discussions of the following sections.

IV. Step-Index Circular Waveguide

In the case of the step-index circular waveguide, i.e., $h(\rho)=0$, the solution of (19) reduces to

$$\Omega^{(n)}(\rho) = AJ_n(h_i\rho) \tag{28}$$

where A is a constant and

$$h_i = \sqrt{k^2\kappa_0^2 - \beta^2}\,. \tag{29}$$

Then, the characteristic equations corresponding to (21)–(24) become

$$\mathrm{HE}_{nm}: \frac{UJ'_{n-1}(U)}{J_{n-1}(U)} - \frac{\kappa_0^2+1}{2} \cdot \frac{WK'_{n-1}(W)}{K_{n-1}(W)} + \frac{n-1}{2}(\kappa_0^2-1) = 0, \qquad n \geqslant 1 \tag{30}$$

$$\mathrm{EH}_{nm}: \frac{UJ'_{n+1}(U)}{J_{n+1}(U)} - \frac{\kappa_0^2+1}{2} \cdot \frac{WK'_{n+1}(W)}{K_{n+1}(W)} - \frac{n+1}{2}(\kappa_0^2-1) = 0, \qquad n \geqslant 1 \tag{31}$$

$$\mathrm{TE}_{0m}: \quad \frac{UJ_0(U)}{J_1(U)} + \frac{WK_0(W)}{K_1(W)} = 0 \tag{32}$$

and

$$\mathrm{TM}_{0m}: \frac{UJ_0(U)}{\kappa_0^2 J_1(U)} + \frac{WK_0(W)}{K_1(W)} = 0 \tag{33}$$

where

$$U = h_i a \qquad W = h_e a. \tag{34}$$

It will be worth mentioning that (32) and (33) are just the rigorous characteristic equations of TE_{0m} mode and TM_{0m} mode, respectively (the case of $l=0$ in (40)). If all the explicitly-appearing κ_0 in (30)–(33) are set equal to one, these equations result in the well-known characteristic equations of LP modes (modes of weakly guiding fiber) [22]; i.e.,

$$\mathrm{HE}_{1m} \to \mathrm{LP}_{0m}: \frac{UJ'_0(U)}{J_0(U)} = \frac{WK'_0(W)}{K_0(W)} \tag{35}$$

$$\mathrm{HE}_{2m}, \mathrm{TE}_{0m}, \mathrm{TM}_{0m} \to \mathrm{LP}_{1m}: \frac{UJ'_1(U)}{J_1(U)} = \frac{WK'_1(W)}{K_1(W)} \tag{36}$$

$$\mathrm{HE}_{n+1,m}, \mathrm{EH}_{n-1,m} \to \mathrm{LP}_{nm}: \frac{UJ'_n(U)}{J_n(U)} = \frac{WK'_n(W)}{K_n(W)}, \qquad n \geqslant 2. \tag{37}$$

All characteristic equations thus far shown were derived assuming such electric fields as (17) and (18). If we use, however, more general expressions like

$$E_{ix} = \sum_{n=0}^{\infty} J_n(h_i\rho)\begin{Bmatrix} C_n \cos n\theta \\ D_n \sin n\theta \end{Bmatrix} \tag{38}$$

$$E_{iy} = \sum_{n=0}^{\infty} J_n(h_i\rho)\begin{Bmatrix} \bar{C}_n \sin n\theta \\ \bar{D}_n \cos n\theta \end{Bmatrix} \tag{39}$$

in (14) and (15), where the upper (lower) terms in (38) and (39) go with each other, we can get the following rigorous characteristic equation of circular dielectric waveguide [23]:

$$\left\{\frac{\kappa_0^2 J'_l(U)}{UJ_l(U)} + \frac{K'_l(W)}{WK_l(W)}\right\}\left\{\frac{J'_l(U)}{UJ_l(U)} + \frac{K'_l(W)}{WK_l(W)}\right\} = \frac{l^2\beta^2}{k^2}\left(\frac{U^2+W^2}{U^2W^2}\right)^2, \qquad l = 0, 1, \cdots. \tag{40}$$

Fig. 3 shows dispersion curves of HE_{11} (LP_{01}) and HE_{12} (LP_{02}) modes of the circular waveguide with $\kappa_0 = 1.5$. The rigorous solutions according to (40) coincide with those according to the approximate equation (30) as long as compared on the graph, while they differ considerably from those according to (35), LP mode approximation. Another illustration of demonstrating high accuracy of equation (30) is Fig. 4, in which relative errors of solutions of (30) and (35) to the rigorous one are compared as a function of κ_0 for HE_{11} mode, using the parameter X, where

$$X = \frac{\kappa_0^2 - (\beta/k)^2}{\kappa_0^2 - 1} = \frac{h_i^2}{h_i^2 + h_e^2}. \tag{41}$$

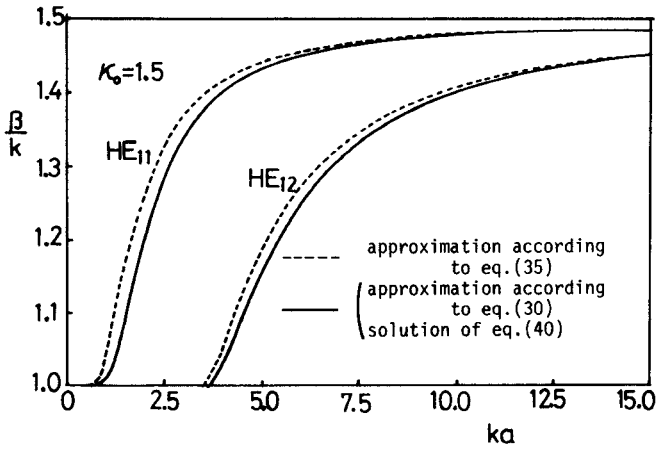

Fig. 3. Dispersion curves of HE_{11} and HE_{12} modes of step-index circular dielectric waveguide. $\kappa_0 = 1.5$.

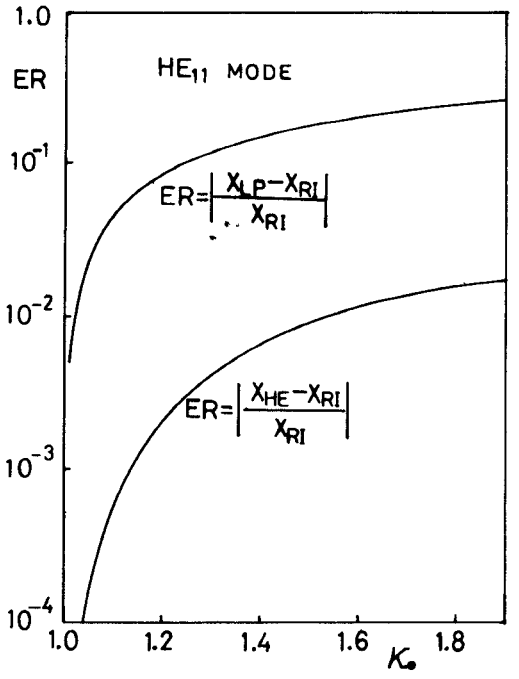

Fig. 4. Comparison of relative errors of approximate propagation constants for HE_{11} mode using the parameter $X\ (=h_i^2/(h_i^2+h_e^2))$. $ka\sqrt{\kappa_0^2-1}=2.0$.

The value of $ka\sqrt{\kappa_0^2-1}$ is chosen as 2.0. X_{HE}, X_{LP}, and X_{RI} correspond to the solutions according, respectively, to (30), (35), and (40). We see that the error of the solution of (30) remains less than 1 percent up to the value κ_0 near 1.6 for this example, whereas in case of the conventional LP mode approximation, κ_0 must be kept less than about 1.02 if the error should be limited within 1 percent.

V. Rectangular Dielectric Waveguide

For the purpose of obtaining solutions as exact as possible, the electric field expansions of (38) and (39) will be well suited also for the rectangular waveguide. In this section, however, we consider another approximation in which the fact is used such that one of two orthogonal components of transverse electric field dominates the other

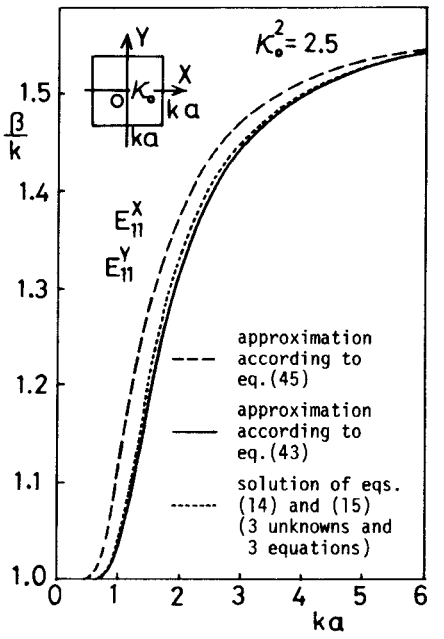

Fig. 5. Dispersion curves of E_{11}^x (or E_{11}^y) mode of square dielectric waveguide. $\kappa_0^2 = 2.5$.

in the case of lower order modes of rectangular dielectric waveguide; i.e., we use the approximation

$$E_{tx}=0 \quad \text{or} \quad E_{ty}=0. \tag{42}$$

Then (14) and (15) are decoupled, resulting in

$$\int_c \left\{ \frac{\partial E_{tx'}}{\partial n'} - E_{tx'} \frac{\partial}{\partial n'} - (\kappa^2-1) E_{ix'} \cos\alpha' \frac{\partial}{\partial x'} \right\} \cdot K_l(h_e\rho') \cos l(\theta'-\theta)\, dv' = 0, \qquad l=0,1,2,\cdots \tag{43}$$

$$\int_c \left\{ \frac{\partial E_{ty'}}{\partial n'} - E_{iy'} \frac{\partial}{\partial n'} - (\kappa^2-1) E_{ty'} \sin\alpha' \frac{\partial}{\partial y'} \right\} \cdot K_l(h_e\rho') \cos l(\theta'-\theta)\, dv' = 0, \qquad l=0,1,2,\cdots. \tag{44}$$

If the explicitly appearing κ are set equal to one in (43) and (44), we finally obtain the equations corresponding to the complete scalar (TEM) approximation or the potential theory [6], which are

$$\int_c \left\{ \frac{\partial E_{tx'}}{\partial n'} - E_{tx'} \frac{\partial}{\partial n'} \right\} K_l(h_e\rho') \cos l(\theta'-\theta)\, dv' = 0, \qquad l=0,1,2,\cdots \tag{45}$$

$$\int_c \left\{ \frac{\partial E_{ty'}}{\partial n'} - E_{iy'} \frac{\partial}{\partial n'} \right\} K_l(h_e\rho') \cos l(\theta'-\theta)\, dv' = 0, \qquad l=0,1,2,\cdots \tag{46}$$

(45) and (46) are the equations that lead to the characteristic equations of LP modes ((35)–(37)), if applied to the case of step-index circular dielectric waveguides [6].

Fig. 5 shows dispersion curves of the E_{11}^x (or E_{11}^y) mode [1], [9] of the square dielectric waveguide with $\kappa_0^2 = 2.5$. The dashed line is the solution of (45) using as E_{tx} the form of (38) with three expansion terms. (The result was checked to be almost the same even if more than four terms were

TABLE I
RELATION BETWEEN THE NUMBER OF EXPANSION AND THE VALUE OF PROPAGATION CONSTANT OF E_{11}^{x} MODE ($ka=3.0$)

NUMBER OF EXPANSION	1	3	5	7	9
COEFFICIENTS	C_0	$C_0\ C_2\ \bar{C}_2$	$C_0\ C_2\ \bar{C}_2$ $C_4\ \bar{C}_4$	$C_0\ C_2\ \bar{C}_2$ $C_4\ \bar{C}_4\ C_6\ \bar{C}_6$	$C_0\ C_2\ \bar{C}_2\ C_4\ \bar{C}_4$ $C_6\ \bar{C}_6\ C_8\ \bar{C}_8$
β/k	1.4455	1.4524	1.4540	1.4542	1.4542

used.) The solid line is the solution of (43) using as E_{tx} the only one term of

$$E_{tx}=C_0J_0(h_t\rho). \tag{47}$$

The dotted line is the solution of a pair of equations (14) and (15) using as E_t both the expansions (38) and (39) but with only three lowest order terms. The reason why the case of only three terms is drawn shall be made clear by Table I in which a state of convergence of β/k is shown as the number of expansion increases; the case of dominant mode and $ka=3.0$ is chosen. The β/k value using electric field consisting of only three terms differs only about 0.12 percent from that using nine terms which could be considered to be rigorous. The solid line corresponds also to the case of one term expansion of Table I. This example suggests that the simple approximation using (43) together with (47) (or (44) together with $E_{ty}=\bar{D}_0J_0(h_t\rho)$) is quite effective to the analysis of the dominant mode even if κ_0 is considerably far from one. Comparison with the results of other references treating rectangular waveguide was not made so exactly, but the results of [1] and [7] seem to almost agree with the solid or the dotted line.

VI. CONCLUSION

A quite general and useful method was presented for analyzing guided modes of dielectric waveguides of arbitrary cross-sectional shape. Basic set of equations which determines the propagation constants and transverse electric field components of modes was derived. This set could be said to be a rigorous equations set, including the case of inhomogeneous-core guides. It was shown by using the examples of circular and rectangular dielectric waveguides that very simple approximate forms for electric fields were sufficient, if used in these rigorous equations, to lead to highly accurate approximations for the propagation constants.

APPENDIX

Elimination of magnetic fields from Maxwell's equations gives

$$\frac{\partial^2E_v}{\partial v\partial n}-\frac{\partial^2E_n}{\partial v^2}-j\beta\frac{\partial E_z}{\partial n}=(k^2\kappa^2-\beta^2)E_n \tag{A1}$$

$$-j\beta\frac{\partial E_z}{\partial v}-\frac{\partial^2E_v}{\partial n^2}+\frac{\partial^2E_n}{\partial n\partial v}=(k^2\kappa^2-\beta^2)E_v \tag{A2}$$

$$j\beta\frac{\partial E_n}{\partial n}+\frac{\partial^2E_z}{\partial n^2}+\frac{\partial^2E_z}{\partial v^2}+j\beta\frac{\partial E_v}{\partial v}=-k^2\kappa^2E_z. \tag{A3}$$

Differentiating (A1) by n and (A2) by v, and summing them we have

$$-j\beta\left(\frac{\partial^2E_z}{\partial n^2}+\frac{\partial^2E_z}{\partial v^2}\right)=2k^2\kappa\left(\frac{\partial\kappa}{\partial n}E_n+\frac{\partial\kappa}{\partial v}E_v\right)+(k^2\kappa^2-\beta^2)\left(\frac{\partial E_n}{\partial n}+\frac{\partial E_v}{\partial v}\right). \tag{A4}$$

Combining (A3) and (A4), we get (8) of the text.

ACKNOWLEDGMENT

The author wishes to thank Prof. N. Kumagai of Osaka University for his constant encouragement, Prof. M. Hashimoto of Osaka Electro-Communication University for valuable discussions and Y. Kume for his help in obtaining numerical results of Sections IV and V.

REFERENCES

[1] J. E. Goell, "A circular-harmonic computer analysis of rectangular dielectric waveguides," *Bell Syst. Tech. J.*, vol. 48, pp. 2133–2160, Sept. 1969.
[2] A. L. Cullen, O. Özkan, and L. A. Jackson, "Point-matching technique for rectangular-cross-section dielectric rod," *Electron. Lett.*, vol. 7, pp. 497–499, Aug. 26, 1971.
[3] J. R. James and I. N. L. Gallett, "Point-matched solutions for propagating modes on arbitrarily-shaped dielectric rods," *Radio Electron. Eng.*, vol. 42, pp. 103–113, Mar. 1972.
[4] E. Yamashita, K. Atsuki, O. Hashimoto, and K. Kamijo, "Modal analysis of homogeneous optical fibers with deformed boundaries," *IEEE Trans. Microwave Theory Tech.*, vol. MTT-27, pp. 352–356, Apr. 1979.
[5] K. Yasuura, K. Shimohara, and T. Miyamoto, "Numerical analysis of a thin-film waveguide by mode-matching method," *J. Opt. Soc. Amer.*, vol. 70, pp. 183–191, Feb. 1980.
[6] L. Eyges, P. Gianino, and P. Wintersteiner, "Modes of dielectric waveguides of arbitrary cross sectional shape," *J. Opt. Soc. Amer.*, vol. 69, pp. 1226–1235, Sept. 1979.
[7] K. Ogusu and K. Hongo, "Analysis of dielectric waveguides by generalized telegraphist's equations," *Trans. IECE Japan*, vol. J60-B, pp. 9–16, Jan. 1977.
[8] H. Shinonaga and S. Kurazono, "Y dielectric waveguide for millimeter- and submillimeter-wave," *IEEE Trans. Microwave Theory Tech.*, vol. MTT-29, pp. 542–546, Jan. 1981.
[9] E. A. J. Marcatili, "Dielectric rectangular waveguide and directional coupler for integrated optics," *Bell Syst. Tech. J.*, vol. 48, pp. 2071–2102, Sept. 1969.
[10] C. G. Williams and G. K. Cambrell, "Numerical solution of surface waveguide modes using transverse field components," *IEEE Trans. Microwave Theory Tech.*, vol. MTT-22, pp. 329–330, Mar. 1974.
[11] M. Matsuhara, "Analysis of TEM modes in dielectric waveguides, by a variational method," *J. Opt. Soc. Amer.*, vol. 63, pp. 1514–1517, Dec. 1973.
[12] R. Pregla, "A method for the analysis of coupled rectangular dielectric waveguides," *Arch. Elektrische Übertragung*, vol. 28, pp. 349–357, Sept. 1974.
[13] E. F. Kuester and R. C. Pate, "Fundamental mode propagation on dielectric fibers of some noncircular cross sections," in *1979 IEEE-MTT Int. Microwave Symp. Dig.*, Apr.–May 1979, pp. 475–477.
[14] C. Yeh, K. Ha, S. B. Dong, and W. P. Brown, "Single-mode optical waveguides," *Appl. Opt.*, vol. 18, pp. 1490–1504, May 15, 1979.
[15] P. C. Waterman, "Scattering by dielectric obstacles," *Alta Frequenza*, vol. 38 (Speciale), pp. 348–352, 1969.
[16] V. K. Varadan and V. V. Varadan, *Acoustic, Electromagnetic and Elastic Wave Scattering-Focus on the T-matrix Approach*. New York: Pergamon, 1980.
[17] N. Morita, "Surface integral representations for electromagnetic scattering from dielectric cylinders," *IEEE Trans. Antennas Propagat.*, vol. AP-26, pp. 261–266, Mar. 1978.
[18] A. W. Snyder and W. R. Young, "Modes of optical waveguides," *J. Opt. Soc. Amer.*, vol. 68, pp. 297–309, Mar. 1978.

[19] H. Kirchhoff, "Wave propagation along radially inhomogeneous glass fibres," *Arch. Elektrische Übertragung*, vol. 27, pp. 13–18, Jan. 1973.
[20] G. L. Yip and S. Nemoto, "The relations between scalar modes in a lenslike medium and vector modes in a self-focusing optical fiber," *IEEE Trans. Microwave Theory Tech.*, vol. MTT-23, pp. 260–263, Feb. 1975.
[21] Y. Kokubun and K. Iga, "Mode analysis of graded-index optical fibers using a scalar wave equation including graded-index terms and direct numerical integration," *J. Opt. Soc. Amer.*, vol. 70, pp. 388–394, Apr. 1980.
[22] D. Gloge, "Weakly guiding fibers," *Appl. Opt.*, vol. 10, pp. 2252–2258, Oct. 1971.
[23] R. E. Collin, *Field Theory of Guided Waves*. New York: McGraw-Hill, 1960, p. 482.

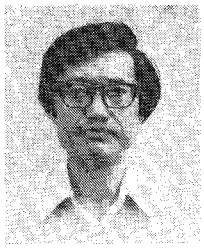

Nagayoshi Morita (M'67) was born in Toyama, Japan, on March 28, 1942. He received B.S., M.S., and Ph.D. degrees in engineering from Osaka University, Suita-shi, Japan, in 1964, 1966, and 1977, respectively.

Since 1966, he has been with the Department of Communication Engineering, Osaka University, Suita-shi, Japan, where he has been engaged in research work on discontinuities in millimeter waveguides and optical waveguides, analytic and numerical techniques for electromagnetic wave problems, bioelectromagnetics, etc.

Dr. Morita is a member of the Institute of Electronics and Communication Engineers of Japan, and Japan Society of Medical Electronics and Biological Engineering.

Refraction at a Curved Dielectric Interface: Geometrical Optics Solution

SHUNG-WU LEE, FELLOW, IEEE, MYSORE S. SHESHADRI, VAHRAZ JAMNEJAD, MEMBER, IEEE, AND RAJ MITTRA, FELLOW, IEEE

Abstract—**The transmission of a spherical or plane wave through an arbitrarily curved dielectric interface is solved by the geometrical optics theory. The transmitted field is proportional to the product of the conventional Fresnel's transmission coefficient and a divergence factor (DF), which describes the cross-sectional variation (convergence or divergence) of a ray pencil as the latter propagates in the transmitted region. The factor DF depends on the incident wavefront, the curvatures of the interface, and the relative indices of the two media. We give explicit matrix formulas for calculating DF, illustrate its physical significance via examples.**

I. Introduction

THE REFRACTION at a dielectric interface is of fundamental importance in electromagnetic theory. If the interface is arbitrarily curved, the only available solution is the one derived by the geometrical optics theory (GO). Such a solution consists of two main ingredients: the well-known Fresnel formulas for the transmission and reflection coefficients (due to A. J. Fresnel in 1823); and a so-called "divergence factor (DF)." Surprisingly, the solution of DF was derived as early as 1915 by Gullstrand [1], but its application was not widely recognized in the electromagnetic/optical community until very recently. In 1972, Deschamps [2], [3] rederived Gullstrand's result by using "curvature matrices" for describing curved surfaces/wavefronts, thus resulting in greater clarity and simpler computations.

In this paper, we supplement Deschamps' results by giving explicit formulas for calculating various curvature matrices and by illustrating the physical significance of DF via analytical and numerical examples. Another motivation for the present work is to compare our solution with the one described by Snyder and Love [4] for the same problem. It is shown that these two solutions are not in agreement.

II. Final Solution for the Refracted Fields

We begin with a statement of the problem. Two infinite dielectric media with refraction indices n_1 and n_2 are separated by a curved interface Σ (Fig. 1), which is described by

$$\Sigma: z = f(x, y). \tag{2.1}$$

The origin of the (x, y, z) coordinates is at the source point 0 in medium 1. The source emits a spherical wave, whose electric field at an observation point $\boldsymbol{r} = (r, \theta, \phi)$ is given by [for $\exp(j\omega t)$ time convention]

$$\boldsymbol{E}^i(\boldsymbol{r}) = \frac{e^{-jk_1 r}}{r}\left[\hat{\theta}P(\theta, \phi) + \hat{\phi}Q(\theta, \phi)\right] \tag{2.2}$$

Manuscript received March 23, 1981; revised July 30, 1981. This work was supported by the Naval Air Systems Command under Contract N00019-79-C-0281.

S. W. Lee, M. S. Sheshadri, and R. Mittra are with the Department of Electrical Engineering, University of Illinois, Urbana, IL 61801.

V. Jamnejad was with the Department of Electrical Engineering, University of Illinois, Urbana, IL 61801. He is now with Jet Propulsion Laboratory, Pasadena, CA 91103.

0018-9480/82/0100-0012$00.75 ©1982 IEEE